CdZnTe Crystal Quality Study by Cathodoluminescence Measurements

Valentin Léger, Thomas Bidaud, Stéphane Collin, Gilles Patriarche, Catherine Corbel, Laurent Rubaldo

CdZnTe CRYSTAL QUALITY STUDY BY CATHODOLUMINESCENCE MEASUREMENTS

Valentin Léger [(1)], Thomas Bidaud [(1)], Stéphane Collin [(1)], Gilles Patriarche [(1)], Catherine Corbel [(2)], Laurent Rubaldo [(3)]

[(1)] C2N, CNRS, Université Paris-Saclay, 10 Boulevard Thomas Gobert, 91120 Palaiseau, France
[(2)] LSI, CEA/DRF/IRAMIS, CNRS, Ecole polytechnique, Institut Polytechnique de Paris, 91120 Palaiseau, France
[(3)] LYNRED, 364 avenue de Valence, 38113 Veurey-Voroize, France
e-mail: valentin.leger@universite-paris-saclay.fr

ABSTRACT

Improving material quality is an essential step to maintain high electro-optical performances at higher operating temperature (HOT) of cooled II-VI infrared (IR) detectors. Indeed, the electrical activity of crystal defects affects their image quality and stability. A first investigation is to correlate the point defect populations with the crystal quality of the $Cd_{1-x}Zn_xTe$ (CZT) substrate, used for the growth of the $Hg_{1-x}Cd_xTe$ (MCT) active layer. For this purpose, spectrally resolved cathodoluminescence (CL) measurements were performed for low and high crystal quality wafers, with a respective dislocation density of 1.8×10^4 cm^{-2} and 6×10^3 cm^{-2}. At 295 K, both wafers showed the band-to-band transition and CL spectra were modeled with the generalized Planck law. However, at 10 K, CL spectra showed that the visibility of phonon replicas of the donor-acceptor pair (DAP) transition at 1.57 eV is dependent on the crystalline order. In addition, the luminescence of the A-center defect ($V_{Cd} - D$) was observed at 1.43 eV only in the low-quality CZT substrate.

Key words: CdZnTe substrate, Cathodoluminescence, Crystal quality, Point defects, A-center, Crystalline order

INTRODUCTION

Cadmium telluride (CdTe) has been extensively studied owing to its interesting material and electrical properties for room-temperature X-ray and γ-ray detectors. By adding an atomic fraction of zinc, the compound $Cd_{1-x}Zn_xTe$ (CZT) made it possible to reach the very high resistivity required for these applications [1]. However, the growth of a high-quality ternary alloy is challenging due to the zinc segregation and the density of extended defects [2].

This difficulty is also encountered in the case of cooled infrared (IR) detectors where CZT is used as a substrate for the growth of the mercury cadmium telluride ($Hg_{1-x}Cd_xTe$ – MCT) active layer, in order to optimize the lattice matching. The crystal quality of the substrate is then a major criterion for the quality of the epitaxial layer. Indeed, the image quality and the stability of the detector are degraded by the electrical activity of crystal defects. In addition, the pixel response is more affected at higher temperature which represents a real issue for the development of II-VI high operating temperature (HOT) technologies.

In this context, improving the material quality is an essential step to maintain high electro-optical performances. A starting point is to investigate and correlate the presence of point defects in substrates with different crystal qualities. Spectrally-resolved luminescence experiments, as photoluminescence (PL) or cathodoluminescence (CL), are very powerful to study radiative mechanisms of carriers via defects [3]. Especially, CL has the advantage of mapping the luminescence properties at the sub-micrometer scale [4].

In this work, CL measurements were made in order to study the luminescence spectra between low and high crystal quality CZT substrates. At 295 K, the band-to-band transition was observed and well fitted by the generalized Planck law, while at 10 K, many transitions occur in the bandgap. Different point defect populations, which are mainly complexes of the cadmium vacancy, can be identified and correlated to the crystal quality of each wafer.

EXPERIMENTAL DETAILS

The $Cd_{1-x}Zn_xTe$ single crystal substrates [5] were grown using the vertical gradient freeze (VGF) technique at LYNRED. The (111) oriented wafers have close composition with low Zn fraction between 3 and 5 atomic percent and are *p*-type conducting with hole concentration of about 10^{15} cm^{-3} at 300 K. They were mechanically polished, chemically etched and stored in air before characterization. Then, 5×5 mm² samples were cut from the 47×48 mm² substrates. The crystal quality of both substrates is characterized by the full width at half maximum (FWHM) calculated for the (222) *X*-ray diffraction peak and the etch pit density (EPD) measured from a neighboring sample of the one used for CL. The low-quality wafer is then distinguished by higher FWHM and EPD values than the high-quality wafer, Table I.

Cathodoluminescence measurements were performed using an Attoligth Chronos CL – scanning electron microscope at 295 K and 10 K. CZT samples were excited by an electron beam with an acceleration voltage of 10 kV and a current of 6 nA. Luminescence was collected by an achromatic reflective objective (numerical aperture 0.72), dispersed with a Horiba diffraction grating (150 grooves/mm and 600 grooves/mm respectively for 295 K and 10 K measurements) and recorded with an Andor Newton charge-coupled-device (CCD) camera (1024×256 pixels, with a pixel width of 26 µm). The corresponding spectral dispersion in the visible to near-infrared range is 0.53 nm per pixel. CL spectra were corrected for the diffraction efficiency of the grating and the sensitivity of the CCD camera. The high stability of the instrument allowed a quantitative comparison of the luminescence of both samples.

At 10 keV, Monte-Carlo simulations using the CASINO software [6] show that 95% of electron-hole pairs are generated in a pear-shaped interaction volume with an approximate depth and width of 240 nm and 210 nm respectively. CL spectra presented in the following sections are mean spectra, averaged over 17×17 µm² CL maps (≥ 128×128 spectra). No extended defect signatures such as dislocations were observed in CL maps. The spectral response recorded for both substrates is then directly obtained from the crystal.

RESULTS AND DISCUSSION

ROOM-TEMPERATURE MEASUREMENTS

Fig.1 shows the CL spectra of high- and low-quality $Cd_{1-x}Zn_xTe$ wafers at room temperature (RT – 295 K). Both substrates exhibit a single broad peak centered at 1.522 eV and 1.527 eV respectively for high- and low-quality, which is near the expected RT bandgap. This characteristic luminescence spectrum is attributed to the band-to-band transition. It can be noticed that the CL intensity is higher for the low-quality wafer. For a given injection level, the CL intensity depends not only on the non-radiative recombination rate, but also on the concentration of free carriers which may differ between the low- and high-quality substrates. As a consequence, the quality of the substrates can not be assessed directly from the luminescence intensity.

The lineshape of the CL spectrum can be modeled with the generalized Planck law. This law is based on the work of Wurfel [7] and has been adapted by Chen et al. [8] to analyze CL spectra of GaAs thin films. The generalized Planck law, equation (1), describes the luminescence spectrum Φ_{lum} at the photon energy $\hbar\omega$ by involving the absorptivity $A(\hbar\omega)$ and the quasi-Fermi levels for electrons and holes $E_{F_{c,v}}$. In equation (2), $R(\hbar\omega)$ is the reflectivity, $\alpha(\hbar\omega)$ is the absorption coefficient and d is a characteristic length over which carriers are generated, travel and recombine radiatively in bulk materials.

$$\Phi_{lum}(\hbar\omega) = \frac{A(\hbar\omega)}{4\pi^2\hbar^3c^2} \cdot \frac{(\hbar\omega)^2}{\exp\left(\frac{\hbar\omega - \left(E_{F_c} - E_{F_v}\right)}{k_B T}\right) - 1} \tag{1}$$

$$A(\hbar\omega) = [1 - R(\hbar\omega)][1 - \exp(-\alpha(\hbar\omega)d)] \tag{2}$$

The modeling of the absorptivity $A(\hbar\omega)$ is the most important part due to its direct dependence on bulk material properties. In the case of an ideal semiconductor, the absorption coefficient denoted α_{ideal} can be described with a parabolic model where no absorption occurs at energies below the bandgap, equation (3).

$$\alpha_{ideal}(\hbar\omega) = \alpha_0 \sqrt{\frac{\hbar\omega - E_g}{E_0 - E_g}} (f_v(E_h) - f_c(E_e)) \tag{3}$$

α_0 is a chosen parameter related to the photon energy E_0. The ideal absorption coefficient is corrected by the occupation probability $f_v(E_h) - f_c(E_e)$, which is related to the excess energy between carriers $\hbar\omega = E_e - E_h$ and weighted according to their effective masses as follows with the parameter w $(0 < w < 1)$: $E_V - E_h = (1 - w)(\hbar\omega - E_g)$ and $E_e - E_C = w(\hbar\omega - E_g)$. In a more realistic case, a sub-bandgap absorption is observed and has

to be considered. This absorption is usually described by an exponential decay called Urbach tail with the energy parameter γ [9]. Thus, the absorption coefficient $\alpha(\hbar\omega)$ is modeled by a convolution of the ideal absorption ($\hbar\omega > E_g$) and the Urbach tail ($\hbar\omega < E_g$), as proposed by Katahara and Hillhouse [10], equation (4).

$$\alpha(\hbar\omega) = \frac{1}{2\gamma} \int_{-\infty}^{\hbar\omega - E_g} \exp\left(-\left|\frac{\varepsilon}{\gamma}\right|\right) \alpha_{ideal}(\hbar\omega - \varepsilon)\, d\varepsilon \quad (4)$$

Finally, the fitting parameters are the bandgap E_g, the temperature T, the characteristic length of carriers d from generation to recombination and the Urbach energy γ. Quasi-Fermi levels are also free parameters, however, the estimation of the injection level indicates that they are away from band edges which makes them undeterminable and have no influence on the modeling. Absorption measurements have not been performed in the studied substrates. Consequently, data from Adachi's work on CdTe has been used for the absorption coefficient ($\alpha_0 = 3.11\times10^4$ cm^{-1} at $E_0 = 1.7$ eV) and the reflectivity $R(\hbar\omega)$ [11]. Regarding the weighting parameter w, $m_{hh}^* = 0.815\, m_0$ and $m_e^* = 0.091\, m_0$ were used [12], leading to a ratio of 0.9.

Fig. 2 shows the luminescence lineshape of the low-quality wafer modeled by the generalized Planck law with a good accuracy over two decades. It can be noticed that calculated parameters, gathered in Table II, are close for both crystal qualities. The fitted bandgap energies are found lower than the expected value and temperature higher than the setpoint of 295 K. Fixing the temperature at the setpoint does not provide a good fit. This suggests that a local heating has to be considered at the surface of the sample due to the electron beam. It is interesting to notice that the point (T, E_g) obtained by the generalized Planck law is in good agreement with the temperature dependence of the bandgap obtained from low-temperature measurements, Fig. 4. Values around 1.8-2 µm have been calculated for d. This result is in agreement with the diffusion lengths reported in the literature: 700 nm to 2.6 µm in the case of p-type CdTe with hole concentration in the 10^{15} - 10^{16} cm^{-3} range [13], and up to 6 µm for 1.5×10^{15} cm^{-3} p-doped CZT [14]. Urbach energies γ are relatively low which indicates a good overall crystal quality. These two last material parameters, d and γ, seem to be independent of the crystal quality.

LOW-TEMPERATURE MEASUREMENTS

Fig. 3 shows the CL spectra of high- and low-quality $Cd_{1-x}Zn_xTe$ wafers at low temperature (LT – 10 K). In contrast with RT measurements, many peaks are observed between 1.35 eV and 1.62 eV. A summary is given Table III. It can be noticed that two differences appear between both crystal qualities. The first point is related to peaks between 1.49 and 1.58 eV which are less visible when the crystal quality is degraded. The second point,

which is the most striking feature, is the presence of the broad structured band around 1.43 eV only for low-quality wafer. In the following, each transition will be discussed, with a particular attention to those that are different between both substrates.

The high-energy part of the spectra is constituted of excitonic transitions with near-band-edge energies. The first one is attributed to the free exciton (FE) recombination. This transition is interesting to estimate the alloy bandgap by adding the binding energy of the exciton around 10 meV, assuming it is very close to that of the binary CdTe [15]. The experimental bandgap measured as a function of the temperature between 10 K and 70 K is shown in Fig. 4 for the low-quality wafer. Data were fitted with the Varshni law [16]. However, the setpoint temperature did not allow to correctly fit the data. The temperature of carriers was therefore extracted from the spectra at $\hbar\omega > E_{FE}$ with a Boltzmann distribution $\exp(-\hbar\omega/k_B T)$ and turned out to be higher than the temperature of the sample holder (33 K and 74 K for 10 K and 70 K respectively). The fitting parameters, given in equation (5), are in good agreement with the previous work of Sánchez-Almazan et al. [17].

$$E_g(T) = 1.6337 - \frac{6.60 \times 10^{-4} \times T^2}{275 + T} \tag{5}$$

At 20 meV from the (FE) transition, the first longitudinal-optical (LO) phonon replica ($FE - 1LO$) appears. The energy difference between both transitions is consistent with that measured by Rowe et al. [18] in the case of CdTe. Their presence is the signature of a good overall crystallinity for both wafers.

Finally, the peaks at 1.614 eV and 1.611 eV, respectively, for low- and high-quality substrates, are associated to the recombination of an exciton bound to an acceptor level (A_1^0X) [13,19-26]. With a localization energy of 5 meV in both substrates, the acceptor level could be related to a residual impurity [19,20] or Cd vacancy complexed with two unknown donors [24].

Luminescence around 1.57 eV is a combination of two transitions although they are difficult to discern in Fig. 3. The first is known as the recombination of an electron from the conduction band to an acceptor level (eA_2^0), and the second, which is 5-6 meV deeper in the bandgap, is the recombination of a donor – acceptor pair (DAP_1) = ($D_2 - A_2$) [22,13,24-28]. It is well established that the acceptor level A_2^0 is common to both transitions, a study as a function of the temperature allows to highlight this characteristic [27,28]. The work of Shin et al. [24] shows that these two transitions disappear from the PL spectra after annealing in Cd atmosphere. From this experiment, the acceptor complex ($V_{Cd} - 2D$) was proposed. As ionization energies (E_{A_2} = 57-58 meV and E_{D_2} = 5-6 meV) calculated in the present work are close to those of Shin et al., the acceptor complex ($V_{Cd} - 2D_1$) is the most probable candidate for A_2^0. However, donors D_1 and D_2 are residual impurities which cannot be identified.

The next three transitions are LO-phonon replicas of the (DAP_1) transition. It is interesting to note that their visibility is degraded in the case of low crystal quality. This feature suggests that the crystalline order of the substrate is, as expected, lower in the low-quality CZT than in the high-quality CZT.

The main contrast between CL spectra concerns the broad luminescence band around 1.43 eV. Indeed, this signal is not observed at all in the high-quality substrate. A fine structure composed of five peaks can be clearly seen. The first is associated to another $(DAP_2) = (D_3^0 - A_3^0)$ transition at around 160 meV under the bandgap and is followed by its LO-phonon replicas. It is accepted that the acceptor level A_3^0 is induced by the so-called A-center defect which is a cadmium vacancy complexed with a donor ($V_{Cd} - D_4$) [28-34]. For intentionally Cl-doped CdTe, the donor implied in the A-center defect is identified as a chlorine atom in a nearby tellurium site [30,34]. CZT wafers studied in this work are undoped, thus, donors D_3 and D_4 are unidentified residual impurities. As this radiative signature only appears in the low-quality wafer, there seems to be a correlation between the formation of A-center defects and the crystal quality of CZT susbtrates.

CONCLUSION

In conclusion, CL measurements at low- and room-temperature have been presented for low and high crystal quality CZT substrates. At 295 K, it was shown that luminescence could be attributed to the band-to-band transition and is well fitted with the generalized Planck law. However, no signature of the crystal quality was found. This result could be developed by adding experimental absorption measurements as input modeling parameters. At 10 K, it has been shown that the visibility of LO-phonon replicas of the (DAP_1) transition is related to the crystalline order of wafers. In addition, the formation of A-center defects was observed only for the low-quality substrate. The crystal quality of the CZT wafers, in terms of EPD and FWHM of the (222) X-ray diffraction peak, can be associated to different populations of point defects.

Although most of the previously observed transitions are due to Cd vacancy complexes, the luminescence of tellurium defects is usually observed with energy levels deeper in the bandgap. Especially, the emission band at 1.1 eV has been attributed to tellurium vacancies [31] or tellurium second phase defects [35-38]. CL measurements in the near-infrared range with a InGaAs camera might help to sort out the discrepancies in this assignment.

	FWHM DDX [arcsec]	Etch pit density [cm^{-2}]
Low-quality wafer	35	1.8×10^{4}
High-quality wafer	23	6×10^{3}

Table I: Values of the full width at half maximum (FWHM) calculated for the (222) *X*-ray diffraction peak and etch pit density (EPD) for low- and high-quality $Cd_{1-x}Zn_xTe$ wafers.

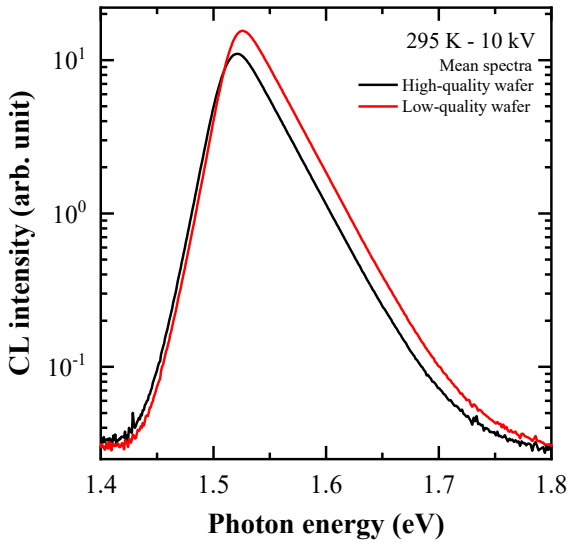

Fig. 1: Cathodoluminescence spectra of low- and high-quality $Cd_{1-x}Zn_xTe$ wafers at room temperature (295 K).

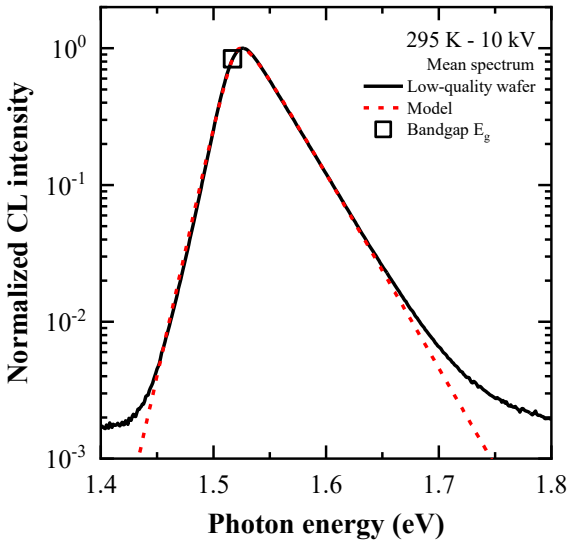

Fig. 2: Cathodoluminescence spectrum of low-quality $Cd_{1-x}Zn_xTe$ wafer (black line) modeled with the generalized Planck law (red dotted line). Fitted parameters are as follow: $E_g = 1.517$ eV, $T = 341$ K, $d = 2$ µm and $\gamma = 8.6$ meV. The calculated bandgap E_g is represented by a black square.

	E_g [eV]	T [K]	d [µm]	γ [meV]
Low-quality wafer	1.517	341	2	8.6
High-quality wafer	1.511	339	1.8	9.1

Table II: Materials parameters calculated from the generalized Planck law for low- and high-quality $Cd_{1-x}Zn_xTe$ wafers.

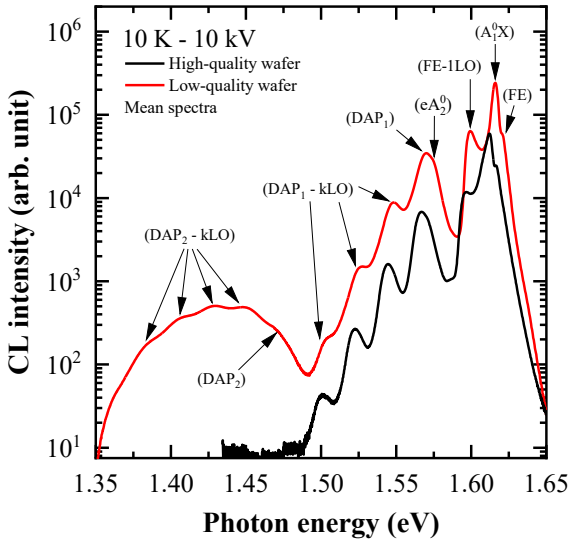

Fig. 3: Cathodoluminescence spectra of low- and high-quality $Cd_{1-x}Zn_xTe$ wafers at low temperature (10 K).

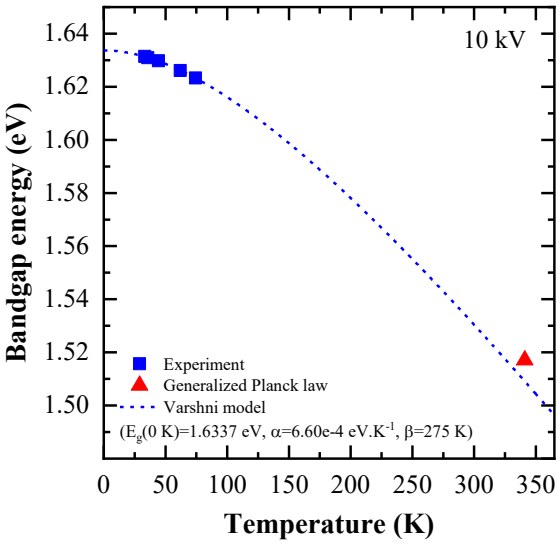

Fig. 4: Modeling of the bandgap energy as a function of the temperature of the low-quality wafer with a Varshni model ($E_g(0\ K) = 1.6337$ eV, $\alpha = 6.60\times10^{-4}$ ev.K^{-1} and $\beta = 275$ K). The red triangle represents the point $E_g(T)$ calculated from the modeling of the room-temperature CL spectrum with the generalized Planck law.

	Low-quality wafer		**High-quality wafer**	
	Transition energy	**Characteristic**	**Transition energy**	**Characteristic**
$\boldsymbol{(FE)}$	1.619 eV	$E_X = 10$ meV (*)	1.616 eV	$E_X = 10$ meV (*)
$\boldsymbol{(A_1^0X)}$ A_1^0: impurity	1.614 eV	$E_{loc} = 5$ meV	1.611 eV	$E_{loc} = 5$ meV
$\boldsymbol{(FE - 1LO)}$	1.599 eV	$E_{LO} = 20$ meV	1.596 eV	$E_{LO} = 20$ meV
$\boldsymbol{(eA_2^0)}$ A_2^0: $(V_{Cd} - 2D_1)$ D_1: impurity	1.573 eV	$E_{A_2} = 58$ meV	1.571 eV	$E_{A_2} = 57$ meV
$\boldsymbol{(DAP_1) = (D_2^0 - A_2^0)}$ D_2^0: impurity	1.568 eV	$E_{D_2} = 5$ meV	1.565 eV	$E_{D_2} = 6$ meV
$\boldsymbol{(DAP_1 - kLO)}$ Phonon replicas	$k = 1$: 1.548 eV $k = 2$: 1.526 eV $k = 3$: 1.503 eV	$E_{LO}^{mean} = 22.5$ meV	$k = 1$: 1.544 eV $k = 2$: 1.522 eV $k = 3$: 1.501 eV	$E_{LO}^{mean} = 21.5$ meV
$\boldsymbol{(DAP_2) = (D_3^0 - A_3^0)}$ A_3^0: $(V_{Cd} - D_4)$ D_3^0, D_4: impurities	1.469 eV	$\hbar\omega = E_g -$ 160 meV	–	–
$\boldsymbol{(DAP_2 - kLO)}$ Phonon replicas	$k = 1$: 1.449 eV $k = 2$: 1.429 eV $k = 3$: 1.407 eV $k = 3$: 1.385 eV	$E_{LO}^{mean} = 21.3$ meV	–	–

Table III: Synthesis of the transitions observed in the CL spectra of low- and high-quality wafers and their respective characteristics at 10 K. (*) From [15].

CONFLICT OF INTEREST

The authors declare that they have no conflict of interest.

REFERENCES

1. Y. Eisen and A. Shor, CdTe and CdZnTe Materials for Room-temperature X-ray and Gamma Ray Detectors. *J. Cryst. Growth* 184-185, 1302 (1998)
2. P. Fougeres, P. Siffert, M. Hageali, J.M. Koebel and R. Regal, CdTe and Cd1−xZnxTe for Nuclear Detectors: Facts and Fictions. Nucl. Instrum. Methods. Phys. Res. A 428, 38 (1999)
3. P.Y. Yu and M. Cardona, Fundamentals of semiconductors: Physics and Materials Properties, 4th ed., (Berlin Heidelberg: Springer-Verlag, 2010)
4. T. Bidaud, J. Moseley, M. Amarasinghe, M. Al-Jassim, W. Metzger and S. Collin, Imaging CdCl2 Defect Passivation and Formation in Polycrystalline CdTe Films by Cathodoluminescence. *Phys. Rev. Mater.* 5, 064601 (2021)
5. B. Pelliciari, J.P. Chamonal, G.L. Destefanis and L. Dicioccio, Growth And Characterization Of LPE CdHgTe/CdZnTe/CdZnTe Structure. Focal *Plane Arrays: Technology and Applications*, Proc. SPIE 0865 (1988)
6. D. Drouin, A.R. Couture, D. Joly, X. Tastet, V. Aimez et R. Gauvin, CASINO V2.42-A Fast and Easy-to-use Modeling Tool for Scanning Electron Microscopy and Microanalysis Users. Scanning 29, 92 (2007)
7. P. Wurfel, The Chemical Potential of Radiation. *J. Phys. C: Solid State Phys.* 15, 3967 (1982)
8. H.L. Chen, A. Scaccabarozzi, R. De Lépinau, F. Oehler, A. Lemaître, J.C. Harmand, A. Cattoni et S. Collin, Quantitative Assessment of Carrier Density by Cathodoluminescence. I. GaAs Thin Films and Modeling. *Phys. Rev. Appl.* 15, 024006 (2021)
9. F. Urbach, The Long-Wavelength Edge of Photographic Sensitivity and of the Electronic Absorption of Solids. Phys. Rev. 92, 1324 (1953)
10. K. Katahara et H.W. Hillhouse, Quasi-Fermi Level Splitting and Sub-bandgap Absorptivity from Semiconductor Photoluminescence. J. Appl. Phys. 116, 173504 (2014)
11. S. Adachi, Optical constants of crystalline and amorphous semiconductors, 1st edn. (Boston, MA: Springer, 1999)
12. P. Capper et J. Garland, Mercury cadmium telluride: Growth, properties and applications, 1st edn. (Wiley, 2010)
13. P. Capper, Properties of narrow gap cadmium-based compounds, 1st edn. (IET, 1994)

14. J. Franc, P. Höschl, E. Belas, R. Grill, P. Hlidek, P. Moravec et J. Bok, CdTe and CdZnTe Crystals for Room Temperature Gamma-ray Detectors. *Nucl. Instrum. Methods Phys. Res. A* 434, 146 (1999)
15. C.E. Barnes and K. Zanio, Photoluminescence in High-resistivity CdTe : In. J. Appl. Phys. 46, 3959 (1975)
16. Y.P. Varshni, Temperature dependence of the energy gap in semiconductors, Physica 34, 149 (1967)
17. F.G. Sánchez-Almazan, H. Navarro-Contreras, G. Ramírez-Flores and M.A. Vidal, Temperature Dependence of the Band Gap of Cd1-xZnxTe Alloys of Low Zinc Concentrations. *J. Appl. Phys.* 79, 7713 (1996)
18. J.M. Rowe, R.M. Nicklow, D.L. Price and K. Zanio, Lattice Dynamics of Cadmium Telluride. Phys. Rev. B 10, 671 (1974)
19. J.P. Chamonal, E. Molva et J.L. Pautrat, Identification of Cu and Ag acceptors in CdTe. *Solid State Commun.* 43, 801 (1982)
20. E. Molva, J.L. Pautrat, K. Saminadayar, G. Milchberg at N. Magnea, Acceptor States in CdTe and Comparison with ZnTe. General Trends. Phys. Rev. B 30, 3344 (1984)
21. S. Seto, A. Tanaka, Y. Masa, S. Dairaku et M. Kawashima, Annealing Behavior of Bound Exciton Lines in High Quality CdTe. Appl. Phys. Lett. 53, 1524 (1988)
22. F.P. Doty, J.F. Butler, J.F. Schetzina et K.A. Bowers, Properties of CdZnTe crystals grown by a high pressure Bridgman method. J. Vac. Sci. Technol. B 10, 1418 (1992)
23. S.P. Tobin, J.P. Tower, P.W. Norton, D. Chandler-Horowitz, P.M. Amirtharaj, V.C. Lopes, W.M. Duncan, A.J. Syllaios, C.K. Ard, N.C. Giles, J. Lee, R. Balasubramanian, A.B. Bollong, T.W. Steiner, M.L.W. Thewalt, D.K. Bowen et B.K. Tanner, A Comparison of Techniques for Nondestructive Composition Measurements in CdZnTe Substrates. J. Electron. Mater. 24, 697 (1995)
24. H.-Y. Shin and C.-Y. Sun, The exciton and edge emissions in CdTe crystals, Mater. Sci. Eng. B Solid. State Mater. Adv. Technol. 52, 78 (1998).
25. S.G. Krylyuk, D.V. Korbutyak, Yu.V. Kryuchenko, I.M. Kupchak et N.D. Vakhnyak, Gamma-radiation Effect on Donor and Acceptor States in CdTe and CdTe:Cl. J. Alloys Compd. 371, 142 (2004)
26. K.D. Glinchuk, A.P. Medvid, A.M. Mychko, YU.M. Naseka, A.V. Prokhorovich et O.M. Strilchuk, Influence of Irradiation with γ-ray Photons on the Photoluminescence of Cd0.9Zn0.1Te Crystals Preliminarily Subjected to the Intense Radiation of a Neodymium Laser. Semiconductors 47, 457 (2013)
27. M. Soltani, M. Certier, R. Evrard et E. Kartheuser, Photoluminescence of CdTe doped with arsenic and antimony acceptors. J. Appl. Phys.78, 5626 (1995)

28. K. Hjelt, M. Juvonen, T. Tuomi, S. Nenonen, E. Eissler et M. Bavdaz, Photoluminescence of Cd1-xZnxTe Crystals Grown by High-Pressure Bridgman Technique. Phys. Status Solidi 162, 747 (1997)
29. B.K. Meyer, W. Stadler, D.M. Hofmann, P. Omling, D. Sinerius et K.W. Benz, On the Nature of the Deep 1.4 EV Emission Bands in CdTe — a Study with Photoluminescence and ODMR Spectroscopy. J. Cryst. Growth 117, 656 (1992)
30. D.M. Hofmann, P. Omling et H.G. Grimmeiss, Identification of the chlorine A center in CdTe. Phys. Rev. B 45, 6247 (1992)
31. D.M. Hofmann, W. Stadler, K. Oettinger, B.K. Meyer, P. Omling, M. Salk, K.W. Benz, E. Weigel et G. Müller-Vogt, Structural Properties of Defects in Cd1-xZnxTe. Mater. Sci. Eng. B 16, 128 (1993)
32. C. Barnett Davis, D.D. Allred, A. Reyes-Mena, J. Gonzalez-Hernandez, O. Gonzales, B.C. Hess et W.P. Allred, Photoluminescence and Absorption Studies of Defects in CdTe and ZnxCd1-xTe Crystals. Phys. Rev. B 47, 13363 (1993)
33. W. Stadler, D.M. Hofmann, H.C. Alt, T. Muschik, B.K. Meyer, E. Weigel, G. Müller-Vogt, M. Salk, E. Rupp et K.W. Benz, Optical Investigations of Defects in Cd1-xZnxTe. Phys. Rev. B 51, 10619 (1995)
34. H.Y. Shin et C.Y. Sun, Photoluminescence spectra of Cl-doped CdTe crystals, Mater. Sci. Eng. B Solid. State Mater. Adv. Technol. 52, 354 (1998)
35. J. Suh, J. Hong, J. Franc, A. E. Bolotnikov, A. Hossain, Ralph B. James, and Kihyun Kim. Tellurium Secondary-Phase Defects in CdZnTe and Their Association With the 1.1-eV Deep Trap. *IEEE Trans. Nucl.* 63, 2657 (2016)
36. A. Wardak, M. Szot, G. Janusz, D. Kochanowska, M. Witkowska-Baran, and A. Mycielski. The 1.1, 0.8 and 0.55–0.60 eV Deep Bands in Detector-grade CdMnTe Studied by Photoluminescence Spectroscopy. *J. of Lumin.* 231, 117833 (2021)
37. A. Mycielski, A. Wardak, D. Kochanowska, M. Witkowska-Baran, M. Szot, R. Jakieła, J.Z. Domagała, L. Kowalczyk, M. Kochański, G. Janusz, M. Dopierała, A. Marciniak, B. Witkowska, B.S. Witkowski, A. Reszka, A. Avdonin, E. Łusakowska, W. Chromiński, M. Lewandowska, and M. Górska. CdTe-based Crystals with Mg, Se, or Mn as Materials for X and Gamma Ray Detectors: Selected Physical Properties. Prog. Cryst. Growth Charact. Mater. 67, 100543 (2021)

38. R. Gul, U. N. Roy, G. S. Camarda, A. Hossain, G. Yang, P. Vanier, V. Lordi, J. Varley, and R. B. James. A Comparison of Point Defects in Cd 1−x Zn X Te 1−y Se Y Crystals Grown by Bridgman and Traveling Heater Methods. J. Appl. Phys. 121, 125705 (2017)